Phenotypic and functional characterization of adult brain neuropoiesis

Bjorn Scheffler*†‡, Noah M. Walton*†, Dean D. Lin§, A. Katrin Goetz*, Grigori Enikolopov¶, Steve N. Roper*§, and Dennis A. Steindler*‡§‖

Departments of *Neuroscience and §Neurosurgery, University of Florida, McKnight Brain Institute, Gainesville, FL 32610; and ¶Cold Spring Harbor Laboratory, Cold Spring Harbor, NY 11724

Communicated by Darwin J. Prockop, Tulane University, New Orleans, LA, May 12, 2005 (received for review January 18, 2005)

The modern concept of neurogenesis in the adult brain is predicated on the premise that multipotent glial cells give rise to new neurons throughout life. Although extensive evidence exists indicating that this is the case, the transition from glial to neuronal phenotype remains poorly understood. A unique monolayer cell-culture system was developed to induce, expose, and recapitulate the entire developmental series of events of subventricular zone (SVZ) neurogenesis. We show here, using immunophentoypic, ultrastructural, electrophysiological, and time-lapse analyses, that SVZ-derived glial fibrillary acidic protein^{low}/A2B5^{+}/nestin^{+} candidate founder cells undergo metamorphosis to eventually generate large numbers of fully differentiated interneuron phenotypes. A model of postnatal neurogenesis is considered in light of known embryonic events and reveals a limited developmental potential of SVZ stem/progenitor cells, whereby ancestral cells in both embryonic and postnatal/adult settings give rise to glia and GABAergic interneurons.

adult stem cells | electrophysiology | *in vitro* | neurogenesis | subventricular zone

Attempts to trace the cellular source of neurogenesis in the adult CNS have recently led to the surprising conclusion that dedicated glial cells give rise to new neurons throughout life (1–5). Even though neurons and glia are both derived from the embryonic neuroepithelium, sharing common signaling pathways and downstream transcription factors during development (6), it is difficult to imagine how one major cell class in the adult brain can transpose into the other. Postnatal neurogenesis in the subventricular zone (SVZ) of rodents proceeds as a characteristic series of events, where multipotent glial cells (referred to as type-B cells) can divide to form colonies of neuroblasts (type-A cells) through a transit-amplifying cell population (type-C cells) (7). Newborn neuroblasts migrate from the SVZ through the rostral migratory stream and mature to GABAergic granule cells and periglomerular cells, which, 3–4 weeks after generation, integrate as inhibitory interneurons into the olfactory bulb of rodents (8–10). Certain features, such as nestin- and glial-fibrillary acidic protein (GFAP) expression, are ascribed to the founder cells of postnatal neurogenesis (3, 11–14), but their distinctive antigenic and functional profiles remain elusive. Traditional approaches for the isolation and characterization of persistent neurogenesis have relied on the *in vitro* neurosphere (NS) assay (15, 16) or on post hoc identification, depending on the incorporation of BrdUrd and/or retroviral constructs to label precursors during cell division. However, neither of these methods affords the recognition of the dynamic processes involved in the maturation of individual cells en route from stem cells to fully differentiated neural phenotypes.

Here, we present an alternative culture model that closely recapitulates *in vivo* postnatal/adult SVZ neurogenesis, allowing us to monitor the entire sequence of hierarchical events from glial-like stem cells to functionally mature (inter)neurons, and to expose the phenotypical and electrophysiological properties of cells in transit.

Materials and Methods

Tissue Culture. SVZ cells from postnatal day 8 (P8) and adult (>90-d-old) animals (C57/B6 mice, The Jackson Laboratory) were placed in DMEM/F-12 (DF) containing 100 units/ml penicillin, 100 μg/ml streptomycin, and 250 ng/ml amphotericin B (collectively, abx), as described in ref. 3. Extracted tissues of five animals were pooled and triturated in 0.005% trypsin (15 min, 37°C, pH 7.3) and placed overnight in uncoated T75 plastic tissue-culture dishes in N5 medium [DF containing N2 supplements, 35 μg/ml bovine pituitary extract, abx, 5% FCS (HyClone), and 40 ng/ml EGF and basic FGF]. Unattached cells were collected, gently triturated by using fire-polished pipettes, replated onto uncoated plastic dishes, and proliferated to confluency in N5 media. EGF and FGF (20 ng each) were added every other day. Confluent cell layers were frozen in aliquots of 1×10^6 cells and maintained in liquid nitrogen. For experimentation, cells were thawed and passaged two or more times by using 0.005% trypsin and N5 media, with 20 ng/ml EGF/FGF supplementation every other day. To induce differentiation, the cells were plated on glass coverslips coated with 10 μg/ml polyornithine (Sigma) and 1 μg/ml laminin (LPO) at densities of $\approx 2 \times 10^5$ cells per cm^2. The cells were proliferated to 90–100% confluency and were induced to differentiate by removing growth factors and serum from the culture media. Dividing cells were labeled with 10 μM BrdUrd (Sigma). Functional neurons were generated by a protocol adapted from Song *et al.* (17). Briefly, retinoic acid (0.5 μM, Sigma) was added between 7 and 10 d after the induction of differentiation and replaced every other day for a period of 6 d. Cytosine β-D-arabinofuranoside (0.5 μM, Sigma) was added for 2 d after the retinoic acid treatment. Neurons were allowed to differentiate in N2-supplemented DF with 0.5% FCS and 20 ng/ml brain-derived neurotrophic factor. The media were changed every other day. Unless otherwise specified, media and growth factors were obtained from Invitrogen and R & D Systems, respectively. Nestin–GFP-expressing animals (18) (age- and sex-matched to C57/B6 mice) were decapitated, and their brains were placed overnight in ice-cold DF containing abx and processed identically. All procedures were approved and performed in accordance with University of Florida Institutional Animal Care and Use Committee guidelines.

Neurosphere Assay. Passage-5 cells from P8 and adult SVZ were trypsinized, counted, and resuspended in nonadhesive six-well plates (Corning) in 2-ml-per-well N5 media containing 1% methylcellulose, as described in refs. 3 and 16. To verify the clonality of NS generated under these conditions, serial dilution of SVZ cells was performed from 0.6 to 20×10^3 cells per cm^2. A linear

Freely available online through the PNAS open access option.

Abbreviations: GFAP, glial fibrillary acidic protein; NS, neurospheres; P8, postnatal day 8; PSA-NCAM, polysialylated neural cell adhesion molecule; SVZ, subventricular zone.

†B.S. and N.M.W. contributed equally to this work.

‡D.A.S. and B.S. are involved with a biotechnology start-up company, RegenMed, Inc., which researches stem cell technology related to human therapeutics.

‖To whom correspondence should be addressed at: McKnight Brain Institute, Program in Stem Cell Biology and Regenerative Medicine, University of Florida College of Medicine, 100 South Newell Drive, P.O. Box 100244, Gainesville, FL 32610. E-mail: steindler@mbi.ufl.edu.

© 2005 by The National Academy of Sciences of the USA

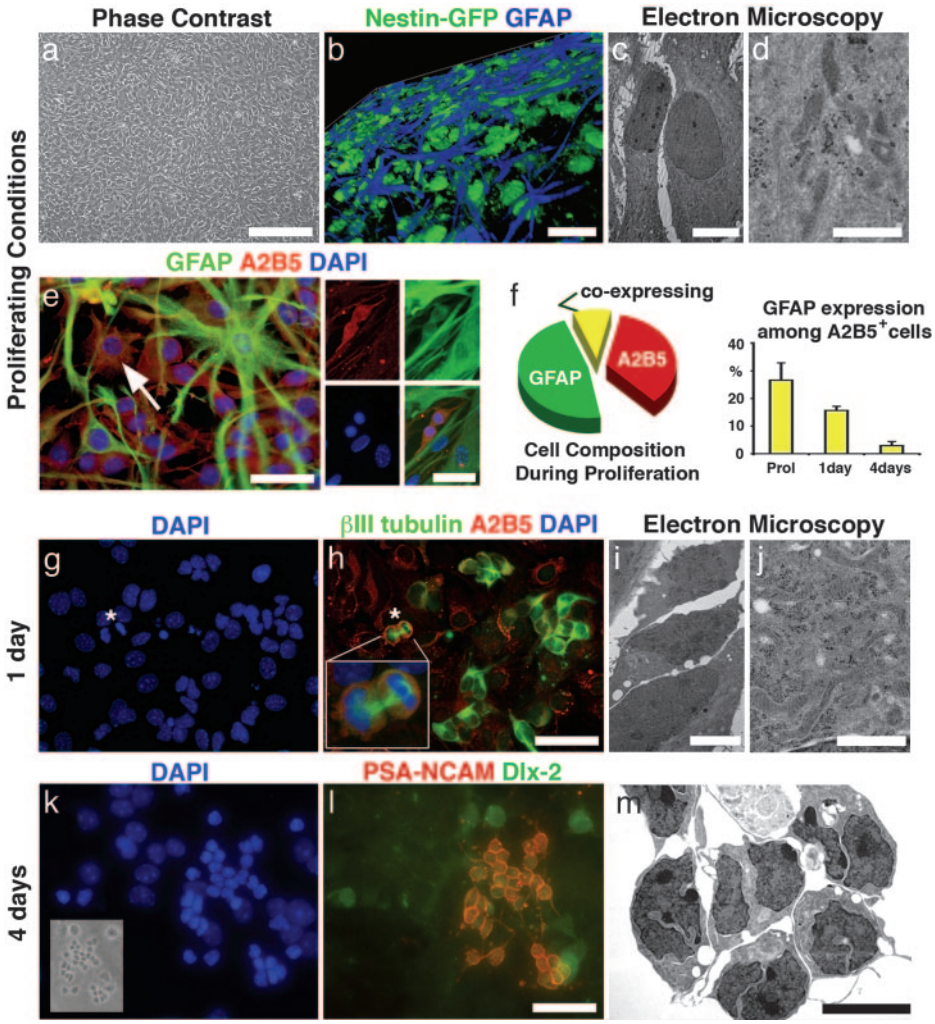

Fig. 1. Monolayers of SVZ cells can be inducibly differentiated into newborn neuroblasts. (*a*) Phase-contrast appearance of a proliferating passage-5 SVZ culture. (*b*) Three-dimensional reconstruction. Large GFAP$^+$ cells overlie compact nestin-expressing cells. (*c* and *d*) Electron micrographs show cells with astrotypic morphology, containing abundant intermediate filaments. (*e*) Low levels of GFAP are found in a subpopulation of underlying nestin$^+$ (image not shown)/A2B5$^+$ cells. The arrow points to a GFAP^{low+}/A2B5$^+$ cell. (*Inset*) One of these cells undergoing division. (*f*) Proliferating SVZ cultures contain 57.3 ± 4.3% GFAP$^+$ and 42.3 ± 1.5% A2B5$^+$ cells. With induced differentiation, GFAP expression among A2B5$^+$ cells (26.6 ± 6.3% during proliferation) decreases sequentially to 15.7 ± 1.5% and 2.9 ± 1.5% at 1 and 4 d after growth-factor withdrawal, respectively. (*g* and *h*) At 24 h after growth-factor removal, differentiating cells display heterogeneous nuclear compaction and transiently co-express A2B5 and βIII tubulin. (*h Inset*) Mitotic cell identified by asterisk in *g*. (*i*) These mitotic cells maintain an intermediate morphology, including cell size and nuclear diameter and display extremely abundant mitochondria and free ribosomes (*j*). (*k*) Defined neuroblasts become abundant 4 d after the initiation of differentiation and are revealed by compacted nuclei and phase-dark morphology (*Inset*). (*l*) Cells are PSA-NCAM$^+$ and weakly Dlx-2$^+$ and are ultrastructurally similar to mixtures of types A and C cells in the SVZ (*m*). [Scale bars (in μm): *a*, 200; *b*, 50; *e*, *h*, and *l*, 30; *c*, 10; *i* and *m*, 5; *d* and *j*, 2.]

seeding/NS relationship was observed at densities between 2.5 and 20×10^3 cells per cm^2 (data not shown). All NS experiments were performed at a seeding density of 10^4 cells per cm^2. To quantify the presence of sphere-forming cells, the total numbers of primary NS were counted per well by using bright-field microscopy ($n = 3$ each for adult and P8 cultures, derived from two independent experiments). Secondary NS were derived from dissociated primary NS and evaluated similarly ($n = 2$ each for adult and P8 cultures, from two independent experiments). NS were evaluated at 14–21 d after cell-seeding. The level of statistical significance was set at $P < 0.01$ and was calculated by using Student's t test. NS were plated on LPO-coated glass coverslips overnight in N5 media. Cells migrating out of NS were allowed to differentiate for 7 d after removing growth factors and serum from the culture media. Individual primary and secondary NS were assessed for multipotentiality by double-immunofluorescence analysis with neuronal (βIII tubulin, MAP 2, and NeuN) and glial (CNPase, GFAP, and O4) marker proteins.

Live Cell Microscopy. Passage-3 SVZ cells were grown to confluency in N5 media on LPO-coated 3-cm glass coverslip dishes (WillCo Wells, Amsterdam). The cells were induced to differentiate, as described above, and were monitored under standard culture conditions (37°C, 5% humidified CO_2) on a Zeiss Cell Observer system. Five randomized visual fields (×200) were selected for analysis 24 h after the induction of differentiation. Phase images were taken every 5 min for up to 30 h. Images were compiled into movies by using the program AXIOVISION (Zeiss).

Electrophysiology. The cells were placed in a holding chamber continuously perfused with oxygenated artificial cerebrospinal fluid containing 125 mM NaCl, 3 mM KCl, 26 mM $NaHCO_3$, 1.25 mM NaH_2PO_4, 20 mM glucose, 1 mM $MgCl_2$, and 2 mM $CaCl_2$ and maintained at 35°C during the experiments. The intracellular pipette solution consisted of 145 mM potassium gluconate, 10 mM Hepes, 10 mM EGTA, and 5 mM MgATP (pH 7.2, osmolarity 290). For experiments in which postsynaptic currents were recorded, 145 mM potassium gluconate was replaced with 125 mM KCl and 20 mM potassium gluconate. Recordings were performed with an Axopatch-1D tight-seal patch clamp (Axon Instruments, Union City, CA) and filtered at 5 kHz. The program CLAMPEX 8.2 (Axon Instruments) was used to deliver command potentials and for data collection. Series resistances were <20 MΩ and were checked frequently to ensure that they did not deviate. For voltage-clamp experiments, a step protocol was applied that held the membrane at potentials between −80 mV and +60 mV for 50 ms after a prepulse period of 200 ms at −100 mV. During current-clamp experiments, a step protocol was used in which currents between 10 and 100 pA per step were applied. The program CLAMPFIT 8.2 (Axon Instruments) was used to analyze voltage and current traces. Picrotoxin was applied at 50 μM, tetraethylammonium chloride was applied at 20 mM, and tetrodotoxin was applied at 400 nM (Alomone Labs, Jerusalem). Chemicals and reagents were ob-

tained from Sigma unless otherwise noted. Data are expressed as mean ± SEM.

Immunocytochemistry. Cells were fixed and processed for immunocytochemistry, as described in ref. 3. Monoclonal antibodies included A2B5 (1:300; Chemicon), βIII tubulin (1:3,000; Promega), BrdUrd (1:50; Becton Dickinson), 2′,3′ cyclic nucleotide 3′-phosphohydrolase (CNPase) (1:250; Chemicon), NeuN (1:50; Chemicon), O4 (1:150; Chemicon), and polysialylated neural cell adhesion molecule (PSA-NCAM) (1:400; Chemicon) and polyclonal antibodies Map-2 (1:30,000; a gift from Gerry Shaw, University of Florida), Dlx-2 (1:50; Santa Cruz Biotechnology), glutamic acid decarboxylase (GAD) 65/67 (1:125; Chemicon), and GFAP (1:600; DAKO), and were detected by using appropriate secondary antibodies (Molecular Probes and The Jackson Laboratory). Secondary antibodies were applied for 45 min at room temperature in PBS, including 0.1% Triton and 10% FCS. Nuclei were visualized by using a 1 μg/ml DAPI stain (Sigma). Fluorescence microscopy was performed and captured on a Leica DMLB upright microscope. Three-dimensional imaging on some specimens was performed by using a fully automated Axiovert 200 inverted microscope equipped with Apotome technology, and images were reconstructed by using the program AXIOVISION (Zeiss).

Electron Microscopy. Passage-3 SVZ cells were grown in N5 media on LPO-coated Aclar coverslips. Fixation and processing were done according to standard protocols. Samples were visualized on a Leica EM10A transmission electron microscope at magnifications between ×1 and ×16,000. Images were captured by using a charge-coupled device digital camera (Finger Lakes Instrumentation, Lima, NY).

Results

To expand a putative SVZ stem-cell population and to remove cells of limited proliferative capacity, single-cell suspensions of microdissected SVZ tissue were proliferated as adherent monolayers for ≥5 population doublings (at least three passages) in 5% serum-containing media supplemented with EGF and FGF (Fig. 1*a*). Cells expressing mature neuronal (NeuN and Map2) or oligodendrocyte (CNPase and O4) markers were not detected in expanded proliferating cultures. Instead, a mixture of mature astrocytes expressing GFAP and immature nestin$^+$ glial phenotypes was present (Fig. 1*b*). The ultrastructural analysis of proliferating cells exposed abundant protoplasmic astrotype morphologies with extensive bundled intermediate filaments (Fig. 1 *c* and *d*). SVZ monolayers could be proliferated for >75 population doublings without senescence and, when transferred to nonadhesive conditions, multipotent primary and secondary neurospheres formed at passage 5 (3.2 ± 0.06% and 0.83 ± 0.25%, respectively) and at passage 25 (4.12 ± 0.79% and 0.81 ± 0.13%) (data not shown). These observations indicate the maintenance of multipotent self-renewing cells in adherent conditions. Further examination of proliferating SVZ cultures revealed a nestin$^+$/A2B5$^+$ population of cells, among which 26.6 ± 6.3% coexpressed low levels of GFAP. These cells showed compact morphologies and, frequently, signs of mitotic activity (Fig. 1 *e* and *e Inset*). The removal of growth factors and serum induced simultaneous differentiation of proliferating cultures and reduced the number of A2B5/GFAP^{low}-expressing cells sequentially (Fig. 1*f*). At the same time, the rapid generation of committed neuronal progeny was observed. At 24 h, glial cells expressing A2B5 and nestin (data not shown) transiently coexpress βIII tubulin (Fig. 1 *g* and *h*), a polycomb gene family member expressed during neuronal fate choice (19, 20). These morphologically unique cells are devoid of GFAP (data not shown) and contain large quantities of mitochondria and ribosomes (Fig. 1 *i* and *j*). Compacted cell colonies appear 3–4 d after growth-factor withdrawal. Individual cells were small and round and ubiquitously

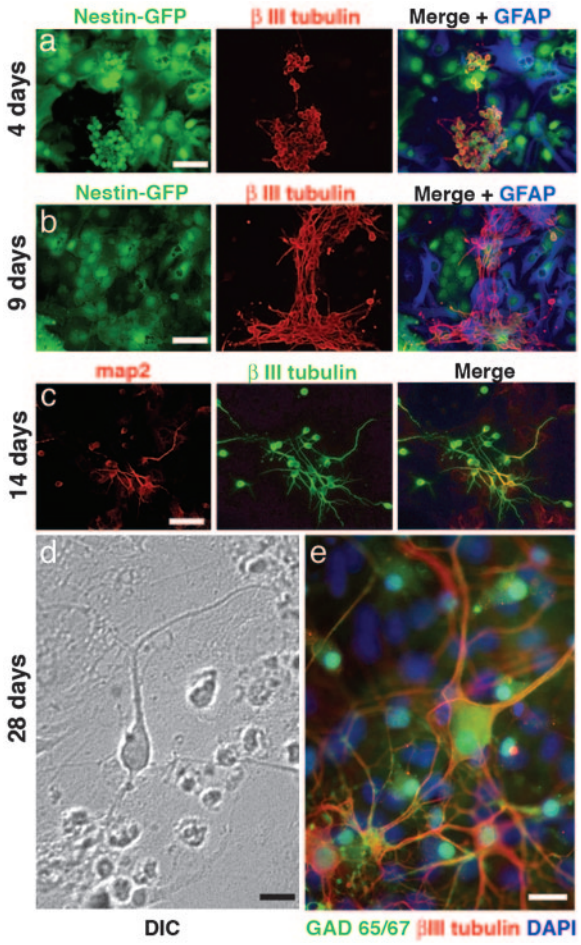

Fig. 2. SVZ-generated neuroblasts develop into interneuron phenotypes. (*a*) Upon appearance, neuroblasts coexpress nestin and βIII tubulin. (*b*) Soon afterward, nestin expression is lost, and bipolar processes are extended. (*c*) Expression of more mature neuronal markers corresponds to increasingly complex neuronal arborization. At 28 d, abundant interneuron phenotypes resemble granule-cell (*d*) and periglomerular (*e*) morphologies, expressing GAD 65/67. [Scale bars (in μm): *a–c*, 25; *d* and *e*, 30.] The number of days indicates time after the induction of differentiation.

expressed βIII tubulin, nestin, and A2B5 (data not shown) as well as PSA-NCAM and low, weak levels of Dlx2 (Fig. 1 *k* and *l*). Phenotypic and ultrastructural hallmarks correspond to mixtures of A and C cells described *in vivo* (21) (Fig. 1*m*). This phenomenon was specific to cultures from the SVZ; characteristic A and C cells could not be derived from cell dissociations of identically prepared parietal neocortex. To evaluate the potential for large-scale production of neuroblasts, confluent monolayers of passage-5 proliferating cells (n = 9, 80,000 cells per cm^2) were differentiated as described above, yielding 39,545 ± 2,691 neuroblasts (βIII tubulin$^+$ cells) per cm^2 4 d after differentiation. These cells are stably maintained in colonies on underlying glia and were easily isolatable for subculture by detachment from underlying cells. Clonally plated cells generated neuroblasts, albeit far less efficiently than did adherent monolayers. Proliferating monolayers also generated CNPase$^+$/O4$^+$ oligodendrocytes (data not shown). To examine the feasibility of developing glial-derived neuroblasts into mature cell types, we induced terminal differentiation using retinoic acid and longitudinally monitored isolated colonies of newborn cells. After their generation, immature A2B5$^+$/nestin$^+$/βIII tubulin$^+$ neuroblasts (Fig. 2*a*) lose nestin antigens and begin to extend bipolar processes (Fig. 2*b*). With time, A2B5 expression is successively

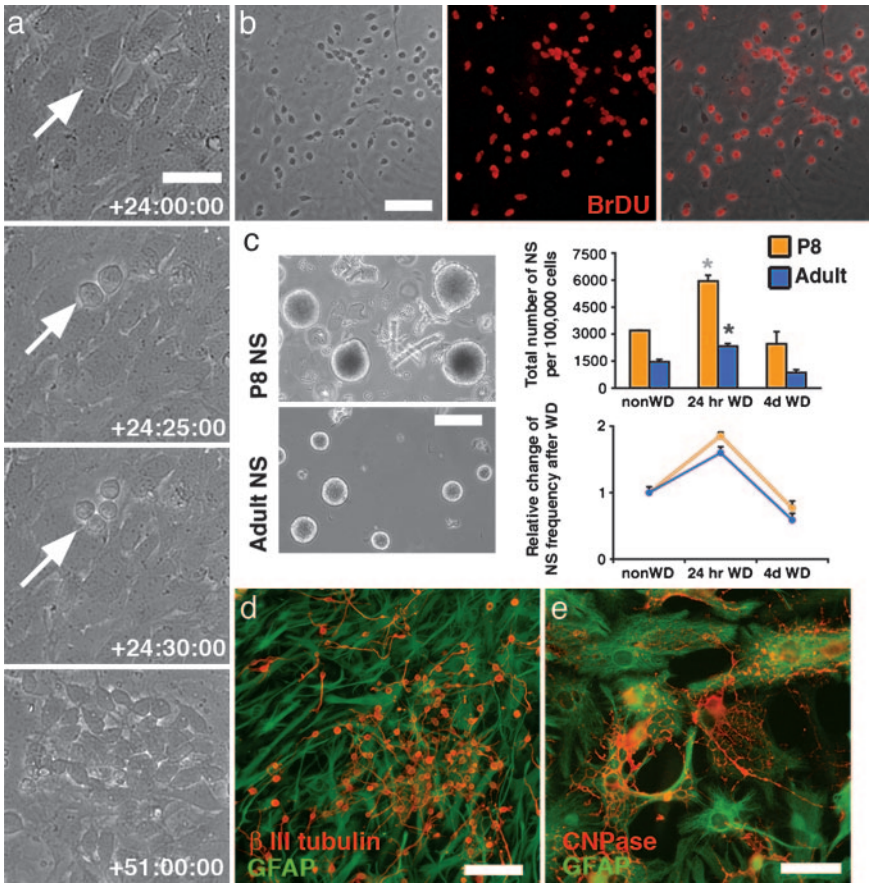

Fig. 3. A mitotically active, multipotent cell emerges transiently during early stages of *in vitro* neuropoiesis. (*a*) Time-lapse microscopy of growth-factor-withdrawn SVZ cultures reveals a transient period, characterized by rapid cell divisions, leading to the initial appearance of neuroblasts within 27 h. (*b*) BrdUrd applied at 48–72 h after the initiation of differentiation labels >95% of all generated neuroblasts. (*c*) Clonal NS were derived from cultured P8 and adult SVZ cells (*Left* for morphological comparison). Total numbers and relative frequencies (*Right*) of NS generated from 100,000 cells per condition increase significantly but transiently at 24 h after growth-factor withdrawal (WD) (*, $P < 0.01$ for adult and P8 compared with non-WD and 4-d WD). (*d* and *e*) Primary and secondary P8 and adult (shown here) neurospheres yield neurons (*d*) and glia (*e*). [Scale bars (in μm): *a*, 15; *b*, 60; *c*, 200; *d* and *e*, 20.]

down-regulated, neuritic arborization becomes increasingly complex, and more mature neuron markers are expressed (Fig. 2*c*; NeuN not shown). At 3–4 weeks after growth-factor withdrawal, characteristic mature interneuronal phenotypes are observed (Fig. 2 *d* and *e*). These neurons almost exclusively express GAD 65/67, a marker for GABAergic interneurons (Fig. 2*e*). Taken together, these results suggest that it is possible to recapitulate and longitudinally track a heteromorphic differentiation process *in vitro* that temporally and phenotypically follows SVZ neurogenesis *in vivo*.

Real-time microscopy was used to capture and characterize the immediate dynamics of localized neurogenic events (Fig. 3*a*). After inducing differentiation, cells maintain a flat, amorphous-glial appearance for 1 d. After this 24-h "silent" period, a sudden, widespread series of rapid cell divisions leads to the initial appearance of neuroblasts. The observed rapid proliferation during this period appears to confirm the ≈12.7-h cell-cycle time reported for the transit-amplifying SVZ population *in vivo* (12). The timing of appreciated mitotic activity is consistent with *in vivo* observations, where ≈50% of putative stem cells are mitotically active 48 h after depleting constitutively proliferating SVZ cells (22). Similar to *in vivo* studies (2), thymidine analog labeling with BrdUrd indicates that the majority of neuroblasts are born 48–72 h after the induction of differentiation (Fig. 3*b*). Our observations of immediate neurogenic events also correlated with the ability of differentiating cells to form clonally derived, multipotent NS (Fig. 3*c*). Adherent cells were trypsinized during proliferation, after 24 and 96 h of growth-factor withdrawal, counted, and plated at clonal density in a conventional NS-forming assay (see *Materials and Methods*). In accordance with findings of decreased neurogenesis in adult brain (23), the total numbers (and diameters) of NS formed in this assay varied with the age of the SVZ tissue. However, a significant and comparably transient increase of the frequency of NS-forming cells was observed regardless of donor brain age at 24 h after induced differentiation (1.86 and 1.6 times in P8- and adult-derived SVZ cultures, respectively). For both age groups, dissociated primary NS yielded clonally derived, multipotent secondary NS (Fig. 3 *d* and *e*), additionally demonstrating the self-renewing potential of rapidly amplifying cells in our culture system.

Whole-cell patch-clamp recordings were used to monitor the longitudinal transition of proliferating SVZ glial cells into mature neuronal phenotypes *in vitro*. Proliferating cells (Fig. 4*a*) displayed a predominance of A-type K^+ currents (IK_A) with hyperpolarized resting membrane potentials. At 1 d after the induction of differentiation, rapidly amplifying cells exhibit low potassium conductances and a predominance of delayed-rectifying K^+ currents (IK_{dr}). At 4 d after induction, membrane properties of clustered newborn cells resemble those of SVZ-born neuroblasts characterized *in vivo* in ref. 24. Neuroblasts present characteristic IK_{dr}, with no significant sodium-channel contribution. Significant changes in passive membrane properties accompany the dramatic morphological transition observed during the first 4 d of differentiation (Fig. 4*b*). After the initial period of rapid change, a second, protracted

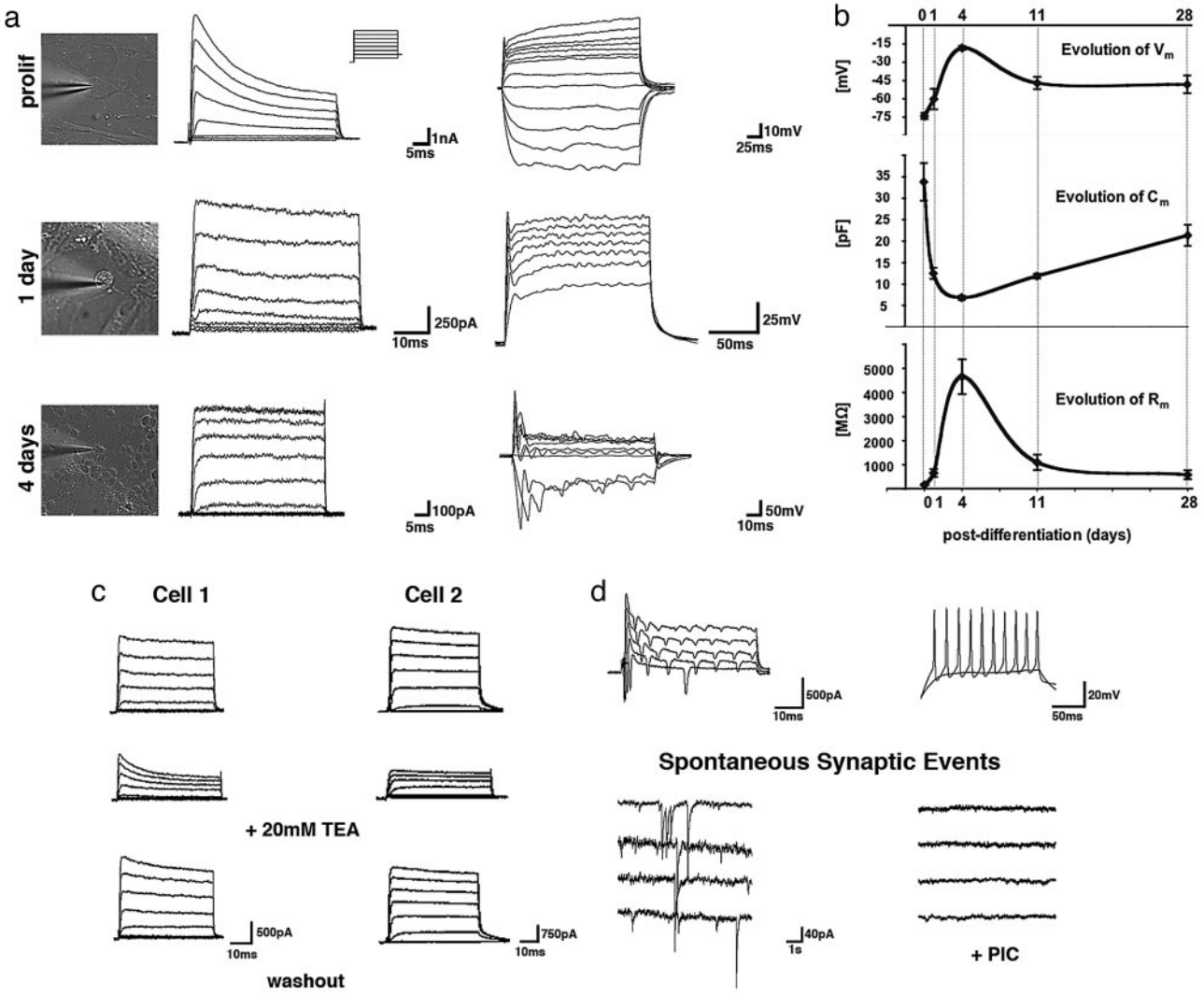

Fig. 4. Differentiating cells recapitulate membrane development consistent with a glial-to-neuron transition. (*a*) Proliferating ($n = 45$), rapidly dividing ($n = 8$), and newborn neuroblast ($n = 20$) cell populations were identified in culture by using infrared differential interference contrast microscopy. Patch-clamp studies (voltage clamp, *Center*; current clamp, *Right*) reveal characteristic changes of functional phenotypes. Cells were incapable of generating action potentials during this period. A small portion (6 of 45) of proliferating cells possessed tetrodotoxin (TTX)-sensitive voltage-gated sodium channels. (*b*) Passive membrane properties (membrane potential, V_m; capacitance, C_m; and input resistance, R_m) during development of SVZ glial cells into functionally mature neuronal phenotypes. (*c*) Voltage-clamp characterization of IK_{dr} 9 d after growth-factor withdrawal ($n = 20$). In some cells (cell 1), tetraethylammonium chloride application exposes underlying IK_A. (*d*) Mature interneurons at 28 days. Glial-derived mature neurons ($n = 14$) fire TTX-sensitive action potentials. Spontaneous synaptic activity can be recorded and entirely blocked by the application of picrotoxin (lower traces). prolif, proliferating; 1 day, rapidly dividing; 4 day, neuroblast.

period of functional neuronal maturation is entered that mimics SVZ neurogenesis *in vivo* (8, 9). This includes gradual repolarization, an increasing membrane capacitance, and a slowly decreasing membrane resistance (Fig. 4*b*). Similar to both *in vitro* (25) and *in vivo* (8) recordings, immature neurons display tetraethylammonium chloride (TEA)-sensitive IK_{dr} at 9 ± 2 d after induction (Fig. 4*c*). In some bipolar cells, the application of TEA exposed underlying IK_A, a typical potassium current of proliferating immature/glial cells (Fig. 4 *a* and *c*). Mature glial-derived neurons (28 ± 4 d) could be elicited to fire series of tetrodotoxin-sensitive action potentials (Fig. 4*d*). Surprisingly, spontaneous synaptic activity consisted almost exclusively of inhibitory events (six of six recorded cells), as demonstrated by the application of picrotoxin, an inhibitor of GABA-mediated synaptic transmission (Fig. 4*d*). This finding suggests that, similar to SVZ neurogenesis *in vivo*, the fate choice of glial-derived neurons *in vitro* is largely restricted to inhibitory phenotypes.

Discussion

The observations presented here expand our and others' previous *in vitro* studies that describe how stem-cell-derived neurons develop basic biophysical characteristics (17, 26–28). Now, we can longitudinally track, *in vitro*, the birth and maturation of precursors specific to the postnatal/adult SVZ, observing the similar timing of developmental events and lineage restrictions as they occur *in vivo*. Moreover, our model offers the advantage of inducible neurogenesis, thereby generating populations of synchronously differentiating SVZ stem cells, which are in monolayers readily available for single-cell analysis in real time throughout early and protracted stages of differentiation. The use of this culture system also enabled us to focus on previously uncharacterized events during the first 96 h of SVZ stem-cell development. $GFAP^{low}/A2B5^{+}/nestin^{+}/\beta III\ tubulin^{-}/Dlx\text{-}2^{-}/PSA\text{-}NCAM^{-}$ proliferating glial cells develop within 24 h into a multipotent, transit-amplifying $GFAP^{-}/A2B5^{+}/nestin^{+}/\beta III\ tubulin^{+}/Dlx\text{-}2^{-/+}/PSA\text{-}NCAM^{-}$ population that

gives rise to GFAP$^-$/A2B5$^+$/nestin$^+$/βIII tubulin$^+$/Dlx-2$^+$/PSA-NCAM$^+$ precursors specific to the SVZ. We present a comprehensive electrophysiological characterization of the glial-to-neuron transition of types B, C, and A cells that closely resembles their transition *in vivo* (7). Significant changes of biophysical properties parallel stage-specific morphological and ultrastructural characteristics of differentiating cells. After induced differentiation, morphologically unique A2B5 cells seem to first lose GFAP, and then nestin, before converting into functionally mature A2B5$^-$ GABAergic interneurons. Thus, the A2B5 antigen, a developmentally regulated tetrasialoganglioside (29), appears to denote the sequential differentiation of a neural stem/progenitor cell en route to becoming an interneuron. Furthermore, we propose that a subpopulation of A2B5$^+$ cells that coexpresses nestin and low levels of GFAP could represent the founders for the SVZ-specific generation of interneurons. Even though the monoclonal antibody A2B5 is not cell-type-specific, because it detects different precursor cells in a variety of developing and adult CNS structures (30–34), we found it intriguing that this antigen is also expressed by a subpopulation of radial glial cells in the lateral ganglionic eminence (LGE) between embryonic days 13.5 and 15.5 (35). The LGE supplies interneurons to the olfactory bulb during brain development (36) and is an ancestor of the postnatal/adult striatal SVZ. In separate pilot studies, we performed immunolabeling on sections of postnatal rat and mouse forebrain (data not shown) and found A2B5$^+$ cells spatially restricted in the dorsolateral (striatal) aspect of the lateral ventricles; this finding could explain, in part, the origin of postnatal interneuron genesis, as we have now completely recapitulated *in vitro*. The use of reductionist culture models remains crucial for uncovering functional aspects of neural and nonneural stem-cell biology (17, 37, 38). Yet, recent studies have indicated that growth factors can significantly change the transcriptional profile of neural precursor cells (39, 40). It is, therefore, a major concern that cellular "reprogramming" induced by EGF, FGF, serum, or other factors influences the behaviors of isolated cells in culture. Of course, cells *in vitro* might not always behave exactly as do their *in vivo* counterparts; however, we demonstrate here that, despite disrupting a system that is clearly based on a large degree of intercellular communication, all characteristic neurogenic events unique to the rodent subventricular zone can be recapitulated in dissociated tissue culture. It can, therefore, be concluded that "organotypic" postnatal neurogenesis does not necessarily require the environmental cues of the host brain. Alternatively, and on a broader perspective, the pioneering work of Dexter *et al.* (41) showed how cells from bone marrow establish themselves in adhesive culture conditions that mimic specific environmental cues for the proliferation and differentiation of hematopoietic cells. Our model could, hence, provide all essential supplies of the environmental niche in the postnatal SVZ, and the results presented here would further support our originally touted similarities between hematopoiesis and neuropoiesis (42).

Uncovering the precise morphogenic cadence during early stages of neuropoiesis, including transitional states and sequential differentiation, as shown here, thus provides insights into, as well as a protocol for, targeted isolation and generation of distinct populations from the spectrum of stem cells to fully differentiated neurons and glia in the adult brain. The SVZ, *in vivo* and *in vitro*, obviously has a propensity to generate GABAergic interneurons. Such a fate restriction associated with the known establishment of a forebrain adult neuronal lineage challenges future research aimed at manipulating neuropoiesis for desired neuronogenesis.

We thank Eric Laywell and Sean Kearns for discussion and technical advice during the course of this work. This work was supported by National Institutes of Health (NIH)/National Institute of Neurological Disorders and Stroke and National Heart, Lung, and Blood Institute Grants NS37556 and HL70143 (to D.A.S.) and NS046384 (to B.S.), an Evelyn F. and William L. McKnight Brain Research Foundation Fund grant (to B.S.), and NIH Training Grant T32HD043730 (to N.W.).

1. Chiasson, B. J., Tropepe, V., Morshead, C. M. & van der Kooy, D. (1999) *J. Neurosci.* **19,** 4462–4471.
2. Doetsch, F., Caille, I., Lim, D. A., Garcia-Verdugo, J. M. & Alvarez-Buylla, A. (1999) *Cell* **97,** 703–716.
3. Laywell, E. D., Rakic, P., Kukekov, V. G., Holland, E. C. & Steindler, D. A. (2000) *Proc. Natl. Acad. Sci. USA* **97,** 13883–13888.
4. Goldman, S. (2003) *Trends Neurosci.* **26,** 590–596.
5. Steindler, D. A. & Laywell, E. D. (2003) *Glia* **43,** 62–69.
6. Rowitch, D. H. (2004) *Nat. Rev. Neurosci.* **5,** 409–419.
7. Doetsch, F. (2003) *Nat. Neurosci.* **6,** 1127–1134.
8. Belluzzi, O., Benedusi, M., Ackman, J. & LoTurco, J. J. (2003) *J. Neurosci.* **23,** 10411–10418.
9. Carleton, A., Petreanu, L. T., Lansford, R., Alvarez-Buylla, A. & Lledo, P. M. (2003) *Nat. Neurosci.* **6,** 507–518.
10. Lois, C. & Alvarez-Buylla, A. (1994) *Science* **264,** 1145–1148.
11. Lendahl, U., Zimmerman, L. B. & McKay, R. D. (1990) *Cell* **60,** 585–595.
12. Morshead, C. M. & van der Kooy, D. (1992) *J. Neurosci.* **12,** 249–256.
13. Gates, M. A., Thomas, L. B., Howard, E. M., Laywell, E. D., Sajin, B., Faissner, A., Gotz, B., Silver, J. & Steindler, D. A. (1995) *J. Comp. Neurol.* **361,** 249–266.
14. Imura, T., Kornblum, H. I. & Sofroniew, M. V. (2003) *J. Neurosci.* **23,** 2824–2832.
15. Reynolds, B. A. & Weiss, S. (1992) *Science* **255,** 1707–1710.
16. Kukekov, V. G., Laywell, E. D., Suslov, O., Davies, K., Scheffler, B., Thomas, L. B., O'Brien, T. F., Kusakabe, M. & Steindler, D. A. (1999) *Exp. Neurol.* **156,** 333–344.
17. Song, H. J., Stevens, C. F. & Gage, F. H. (2002) *Nat. Neurosci.* **5,** 438–445.
18. Mignone, J. L., Kukekov, V., Chiang, A. S., Steindler, D. & Enikolopov, G. (2004) *J. Comp. Neurol.* **469,** 311–324.
19. Cai, L., Morrow, E. M. & Cepko, C. L. (2000) *Development (Cambridge, U.K.)* **127,** 3021–3030.
20. Dennis, K., Uittenbogaard, M., Chiaramello, A. & Moody, S. A. (2002) *Gene* **294,** 269–277.
21. Doetsch, F., Garcia-Verdugo, J. M. & Alvarez-Buylla, A. (1997) *J. Neurosci.* **17,** 5046–5061.
22. Morshead, C. M., Reynolds, B. A., Craig, C. G., McBurney, M. W., Staines, W. A., Morassutti, D., Weiss, S. & van der Kooy, D. (1994) *Neuron* **13,** 1071–1082.
23. Kuhn, H. G., Dickinson-Anson, H. & Gage, F. H. (1996) *J. Neurosci.* **16,** 2027–2033.
24. Wang, D. D., Krueger, D. D. & Bordey, A. (2003) *J. Neurophysiol.* **90,** 2291–2302.
25. Stewart, R. R., Zigova, T. & Luskin, M. B. (1999) *J. Neurophysiol.* **81,** 95–102.
26. Strubing, C., Ahnert-Hilger, G., Shan, J., Wiedenmann, B., Hescheler, J. & Wobus, A. M. (1995) *Mech. Dev.* **53,** 275–287.
27. Finley, M. F., Kulkarni, N. & Huettner, J. E. (1996) *J. Neurosci.* **16,** 1056–1065.
28. Benninger, F., Beck, H., Wernig, M., Tucker, K. L., Brustle, O. & Scheffler, B. (2003) *J. Neurosci.* **23,** 7075–7083.
29. Eisenbarth, G. S., Walsh, F. S. & Nirenberg, M. (1979) *Proc. Natl. Acad. Sci. USA* **76,** 4913–4917.
30. Raff, M. C., Miller, R. H. & Noble, M. (1983) *Nature* **303,** 390–396.
31. Rao, M. S., Noble, M. & Mayer-Proschel, M. (1998) *Proc. Natl. Acad. Sci. USA* **95,** 3996–4001.
32. Mi, H. & Barres, B. A. (1999) *J. Neurosci.* **19,** 1049–1061.
33. Noble, M., Arhin, A., Gass, D. & Mayer-Proschel, M. (2003) *Dev. Neurosci.* **25,** 217–233.
34. Nunes, M. C., Roy, N. S., Keyoung, H. M., Goodman, R. R., McKhann, G., II, Jiang, L., Kang, J., Nedergaard, M. & Goldman, S. A. (2003) *Nat. Med.* **9,** 439–447.
35. Li, H., Babiarz, J., Woodbury, J., Kane-Goldsmith, N. & Grumet, M. (2004) *Dev. Biol.* **271,** 225–238.
36. Wichterle, H., Garcia-Verdugo, J. M., Herrera, D. G. & Alvarez-Buylla, A. (1999) *Nat. Neurosci.* **2,** 461–466.
37. Colter, D. C., Sekiya, I. & Prockop, D. J. (2001) *Proc. Natl. Acad. Sci. USA* **98,** 7841–7845.
38. Shen, Q., Goderie, S. K., Jin, L., Karanth, N., Sun, Y., Abramova, N., Vincent, P., Pumiglia, K. & Temple, S. (2004) *Science* **304,** 1338–1340.
39. Gabay, L., Lowell, S., Rubin, L. L. & Anderson, D. J. (2003) *Neuron* **40,** 485–499.
40. Hack, M. A., Sugimori, M., Lundberg, C., Nakafuku, M. & Gotz, M. (2004) *Mol. Cell. Neurosci.* **25,** 664–678.
41. Dexter, T. M., Allen, T. D. & Lajtha, L. G. (1977) *J. Cell. Physiol.* **91,** 335–344.
42. Scheffler, B., Horn, M., Blumcke, I., Laywell, E. D., Coomes, D., Kukekov, V. G. & Steindler, D. A. (1999) *Trends Neurosci.* **22,** 348–357.